Arch. Min. Sci. **68** (2023), 3, 409-423

Electronic version (in color) of this paper is available: http://mining.archives.pl

DOI: https://doi.org/10.24425/ams.2023.146859

YULONG LIU[1,2], LEI HUANG[2], GUICHENG HE[1], NAN HU[1], SHUHUI ZHOU[2], QING YU[1], DEXIN DING[1*]

DAMAGE AND STABILITY ANALYSIS OF SANDSTONE-TYPE URANIUM ORE BODY UNDER PHYSICAL AND CHEMICAL ACTION OF LEACHING SOLUTION

In this paper, the typical sand-conglomerate uranium ore in north China was taken as the research object. The uniaxial compression and tensile tests of sand-conglomerate specimens under natural status and acidic solution status were used to research the compressive strength, tensile strength, Young's modulus, cohesion and internal friction angle. Focusing on this type of uranium deposit, during the underground design of the in-situ leaching mining method, the three-dimensional finite element method was used to conduct a numerical simulation of the liquid collecting tunnel with different structural parameters of 10 m×2 m, 3 m×2 m, 2 m×2 m, and comprehensively analyse the vertical displacement, principal stress and plastic deformation zone changes of the tunnelbefore and after leaching. Based on the results, influenced by an acidic aqueous solution, the grain of the conglomerate became soft and secondary pores appeared, resulting in the superimposed effect of physical damage and chemical damage. Macroscopically, an obvious decrease was witnessed in mechanical property. Based on the stability and economy factor of three scenarios before and after leaching, the scenario was recommended as the experimental testing scenario, specifically, two longitudinal collecting tunnel were arranged along the strike of the orebody, with the size of 3 m×2 m and the width of the middle pillar of 4 m. The results of the numerical simulation are significant in guiding the design of underground in-situ leaching technology and determining the structural parameters of the deposit.

Keywords: Numerical simulation; Stability analysis; Underground in-situ leaching; Physicochemical interaction; Collecting tunnel

1. Introduction

In recent years, Uranium geologists in China have discovered a type of strongly weathered and oxidised sandstone uranium deposit with steep inclined and drainage in the north sandstone

[1] KEY DISCIPLINE LABORATORY FOR NATIONAL DEFENSEFOR BIOTECHNOLOGY IN URANIUM MINING AND HYDROMETALLURGY, UNIVERSITY OF SOUTH CHINA, CHINA

[2] CHINA GENERAL NUCLEAR POWER GROUP (CGN) URANIUM RESOURCES CO., LTD, BEIJING 100029, CHINA

* Corresponding author: dingdxzzz@163.com

uranium metallogenic belt [1]. The main characteristics of this type of uranium deposit are that it has experienced the process of orogenic uplift and denudation with multiple periods of pulsation, the deposit is steeply inclined, and the ore-bearing aquifer has been drained by the tectonic belt formed by geological action, and the sandstone uranium ore has evolved into highly weathered and oxidised sandstone uranium ore under the action of the external atmosphere. According to the hydrogeological conditions of the deposit, it can not be mined by the in-situ leaching method, and it is difficult to be mined by the in-situ blasting leaching method because the ore body and surrounding rock are very unstable. Therefore, the new technology of underground in-situ leaching is proposed to exploit this type of uranium deposit safely, economically and environmentally. This kind of technique has not been found in other literature yet. Fig. 1 is a typical scheme diagram of the underground in-situ leaching process. Its structural parameters include layering height (H), spacing of liquid distribution (collecting) tunnels (B) and size of liquid distribution (collecting) tunnels (height H and width B). The upper and lower tunnels for collecting and distributing liquid can be used interchangeably. The structural parameters, particularly the size and spacing of the tunnels, have a significant impact on the in-situ leaching engineering, pipeline layout, and stope stability. These parameters also greatly affect the safety and profitability of the mining process.

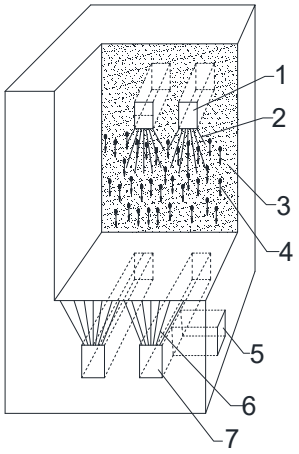

1 – liquid distribution tunnel; 2 – Liquid distribution drilling; 3 – Loose ore body; 4 – Flow direction of leaching solution; 5 – Liaison tunnel; 6 – Collecting hole; 7 – Liquid collecting tunnel

Fig. 1. Typical scenario of underground in-situ leaching mining method

It is necessary to solve the problem of stope stability induced by rock strength weakening after water-rock interaction through theoretical research and experimental verification to adopt underground in-situ leaching technology and technology to mine steeply-inclined dredged highly weathered and oxidised sandstone uranium deposits, to popularise it in design and production stage. The study of water-rock interaction by domestic and foreign scholars shows that the weakening effect of water on rock mass is very apparent. Sun Jun [2] showed that the long-term compressive strength of red sandstone under saturated conditions was only about 50% of that under dry conditions. Zhu Hehua et al. [3] conducted a comparative study on uniaxial creep of tuff under dry and saturated conditions, which showed that the limit creep values were 5-6 times different

under dry and saturated conditions. Li Peng et al. [4] showed that a hydrochemical solution could significantly reduce the shear strength of sandstone, and the concentration of the acidic solution was positively correlated with the shear strength of sandstone. The research results of Liu Jian et al. [5] show that the creep rate of saturated sandstone is higher than that of dry sandstone, and the creep is time-sensitive. Tang Liansheng et al. [6-9] discussed the failure mechanism of rock mass after water-rock chemical interaction, indicating that rock damage is closely related to the strength of chemical interaction. Cui Qiang et al. [10] studied the influence of chemical corrosion on sandstone porosity and established the relationship of porosity changing with time under the action of the solution. The study of Wang Wei et al. [11] shows that during the interaction between acidic solution and sandstone, solution pH gradually tends to be neutral, and sandstone strength decreases. Hongdi Jing et al. [12] utilised SEM electron microscopy and X-ray to study the stability of expansive soft rock roadway, revealed that water swelling can cause considerable deformation to the roadway. Other scholars [13-17] established a model of rock damage underwater physicochemical action through experimental research, providing a calculation basis for the variation of mechanical parameters such as stress intensity factor after water-rock interaction in the engineering rock mass. It is necessary to carry out the change of physical and mechanical parameters of sandstone before and after in-situ leaching, which can provide necessary mechanical parameters for the numerical simulation of stope stability.

With the development of computer technology, finite element numerical simulation technology has been rapidly developed and applied in the field of mining engineering. Zhou Zonghong et al. [18-19] used three-dimensional finite element numerical simulation method to analyse the deformation and damage mechanism of the roof slab rock in the empty zone and proposed corresponding control methods; Tao Ganqiang et al. [20] used three-dimensional finite element method to numerically simulate the stability of the cave-in method with different structural parameters of the quarry, analysed the vertical displacement and main stress change law of the roof slab of the tunnel in two different processes of approach excavation and ore recovery, and proposed safe and reliable structural parameters of the quarry; Gong Jian et al. [21] established a mechanical model of the cave-in zone, analysed the stress state of the roof plate of the mining area, simulated the stress situation of the mining area using a three-dimensional finite element model, and successfully predicted the location and timing of the cave-in of the mining area; Zhang Yaoping et al. [22] used a three-dimensional finite element method to simulate, calculate and predict the stability of the empty zone formation and the mining area in Longqiao iron ore mine, and effectively derived displacement situation and stress state around the mining hollow area, which provides an important basis for controlling hazardous ground pressure activities at the mine site. In addition to computer numerical simulation, some scholars also use CCD (charge-coupled device) camera technology [23] and traditional monitoring and measurement technology to measure and study the deformation of underground space structures [24].

This paper takes the Sawafuqi uranium deposit as a studied object, uses the finite element numerical simulation method, and mainly simulates the changes of displacement, stress and plastic damage of the top and bottom plate of the liquid distribution (collector) liquid tunnel before and after leaching. Analyses are made on the influence law of structural parameters on the stability of the tunnel and provide the theoretical basis for the design of structural parameters of production practice quarries.

The Sawafuqi uranium deposit is located in the intermountain basin of the Kuergan formed by the South Tianshan orogenic belt at the northern edge of the Tarim Basin. The deposit is

mainly in the middle of the iconic coal seam of the Tiemiersu Group of the Lower Middle Jurassic Klasu Group, and the rock type is predominantly sand and conglomerate, whilst the ore body is laminated, laminar-like and plate-like [25], as shown in Fig. 2. The deposit is nearly east-west trending, about 950 m long along strike, extending 380 m-500 m in southwest trend, with an average thickness of 10 m and a burial depth of about 570 m at a shallow dip angle of 50°-80°. The top and bottom plates of the uranium deposit are muddy sandstone or sandy mudstone with poor permeability, which can be used as an effective water barrier for in-situ leaching mining underground.

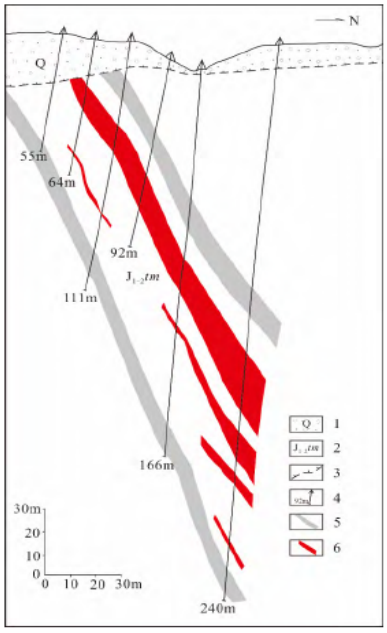

1 – Quaternary sedimentary layer; 2 – Timirsu Formation; 3 – Unconformity surface; 4 – Borehole and hole depth; 5 – Coal seam; 6 – Uranium ore body

Fig. 2. The ore body shape of Sawafuqi uranium deposit

2. Test and simulation methods

2.1. Rock structure and mineral composition test process

The ore samples were prepared and put into the Mineral Liberation Analyser (MLA), X-ray Back Scattered Electron Analysis Mode (XBSE) and Sparse Phase Lite X-ray Back Scatter Analysis Mode (SPL_XBSE) were used to analyse the samples to determine the main mineral composition, dissociation status of uranium minerals and co-occurrence of uranium minerals with other minerals. At the same time, the uranium samples were characterised by scanning electron microscopy and energy spectrum to observe the microstructure and qualitative analysis of its elemental composition.

2.2. Rock physical and mechanical properties test process

The specimens were processed, and standard cylindrical specimens were prepared according to the test protocol for the physical and mechanical properties of rocks [26]. Firstly, the wave velocities of all specimens were tested, and the specimens with good uniformity were selected to carry out the relevant tests. Secondly, the specimens were dried in a constant-temperature drying oven, and after cooling, the specimens were divided into two equal batches, one as is and the other immersed in a weak acid solution under evacuation for 4 hours until saturation. The RMT-150B electro-hydraulic servo rock mechanics test system was used to test the compressive strength, tensile strength and shear strength of the specimens in the original and saturated samples, and three parallel samples were made for each group of samples to obtain the uniaxial compressive strength, uniaxial tensile strength, modulus of elasticity E and Poisson's ratio μ of the specimens, the loading rate is 0.002 mm/s, the dimensions of the sample is 50 mm and 101 samples were tested in total.

2.3. Numerical simulation of quarry stability

2.3.1. Calculation model

The FLAC3D software was used to analyse the influence of structural parameters on the stability of the mining site, using an underground in-situ leaching field as the research object. According to the theory of elasto-plasticity mechanics, the model range used for calculation is 3-5 times the range of the mining area in order to calculate the need and high calculation accuracy. The length × width × height of the calculation model is 190 m×10 m×120 m respectively, that the length along the strike of the ore body is taken as 10 m, the width along the tendency of the ore body is taken as 190 m, the height in the vertical direction is taken as 120 m and the depth of the ore body is 400 m. The grid is finer in the mining area and its vicinity, while a sparse grid is used outside the area, which can reduce the number of nodes and cells, making the calculation results more accurate. The entire model is divided into 188,760 eight-node isoparametric cells, with a total of 19,7715 nodes. Since the range of mining influence is limited, the displacement values farther away from the surrounding rock will be small and tend to be zero. Therefore, the model boundary is constrained by displacement, i.e., the bottom surface of the model is fully constrained, and the four sides of the model are restricted to move in the horizontal direction perpendicular to this plane.

2.3.2. Calculation method

Since the study area is a sandstone uranium deposit with good continuity and undeveloped tectonic-like structures, the study area can be considered to be in a uniform stress field, so the vertical and horizontal stresses caused by the weight of the overlying rock are calculated by the following equations, respectively.

$$\sigma_z = \gamma H \tag{1}$$

$$\sigma_x = \sigma_y = \frac{\mu}{1-\mu}\gamma H \tag{2}$$

In the above equation: γ is the capacitance of sandstone; μ is the Poisson's ratio of the rock; H is the burial depth of the rock body.

In rock failure analysis, the Mohr-Coulomb criterion is used to analyse the extent of rock failure and yield conditions.

$$f_s = \sigma_1 - \sigma_3 \frac{1+\sin\varphi}{1-\sin\varphi} - 2c\sqrt{\frac{1+\sin\varphi}{1-\sin\varphi}} \tag{3}$$

In the above equation: σ_1 and σ_3 are the maximum principal stress and minimum principal stress, respectively, c is the cohesion of the rock, φ is the angle of internal friction of the rock, and f_s is the judgement coefficient of rock damage. When $f_s \geq 0$, shear damage will occur in the rock.

The rock is in a state of tensile stress, and the tensile breaking strength criterion is used to determine the rock yield conditions.

$$f_s = \sigma_t - R_t \tag{4}$$

In the above equation: σ_t is the tensile stress to which the rock is subjected, and R_t is the tensile strength of the rock. If the tensile stress is greater than the tensile strength of the rock, the rock will be broken.

2.3.3. Mechanical parameters

According to the geological conditions and the actual situation of the mine, the ore rocks are simplified into three basic models: cover, coal seam and sand conglomerate (containing ore seam). The engineering geology report was used to select the mechanical parameters for both the quaternary cover and coal seam. The mechanical parameters of the sand conglomerate ore body are based on the test data, and the rock mechanics are appropriately modified according to the rock mass classification method by considering the structural effects of the rock body, and the values are taken as shown in TABLE 1.

TABLE 1

Physical mechanical parameters of sand conglomerate before and after leaching

Type	Density / (g/cm^3)	Compressive strength / MPa	Tensile strength / MPa	Modulus of elasticity / GPa	Poisson's ratio	Internal friction angle / °	Cohesive force / MPa
Cover seam	1.96	3.50	0.35	0.25	0.35	25	0.35
Coal seam	1.40	8.95	0.50	0.99	0.31	28	1.05
Sand conglomerate (before leaching)	2.40	17.37	1.06	1.97	0.31	32	1.71
Sand conglomerate (after leaching)	2.45	13.23	0.86	1.62	0.32	31	1.42

2.3.4. Calculation scheme

In the underground in-situ leaching mining process, the stability of the bottom collecting tunnel is a crucial condition for safe production. By considering the thickness of the ore body, dip angle and other endowment states, three different structural parameters of the liquid collecting tunnel are designed. Moreover, the distribution and changes of mechanical parameters

such as maximum principal stress, minimum principal stress, displacement and the plastic zone around the tunnel before and after leaching are calculated by numerical simulation to analyse the stability of the mining site. No support structures were applied. A scenario of the collecting tunnel layout is shown in Fig. 3.

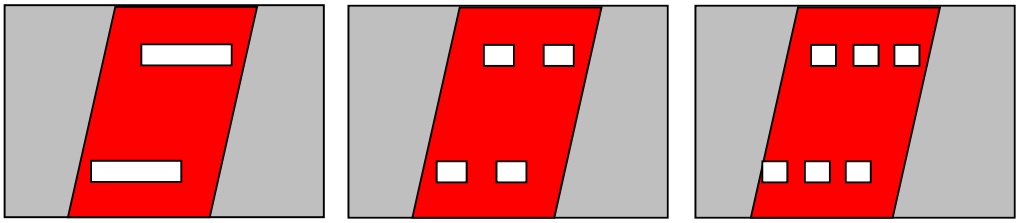

Scheme I: One liquid collecting tunnel is arranged along the strike of the ore body, with tunnel width W = 10 m and height H = 2 m

Scheme II: Two liquid collecting tunnels are arranged along the strike of the ore body, with the width of the tunnels W = 3 m, height H = 2 m, and the width of the central pillar 4 m

Scheme III: Three liquid collecting tunnels along the strike of the ore body, with a width of W = 2 m, a height of H = 2 m and a central pillar width of 2 m

Fig. 3. Scenario of collecting tunnel layout

3. Results and discussion

3.1. Rock structure and mineral composition results and analysis

The rock sample used for the test was a sand conglomerate from the Sawafuqi uranium mine in Xinjiang. The rocks consist mostly of quartz, rock fragments, feldspar, and clastic cement. The quartz is mainly polycrystalline quartz and monocrystalline quartz; the rock debris is mainly volcanic clastic rock, followed by a small amount of schist debris. The rock sample is a gravelly structure with sub-angular to sub-rounded grains and porous cementation. Microstructure images of the rock samples are shown in Fig. 4. The minerals that are closely associated with uranium

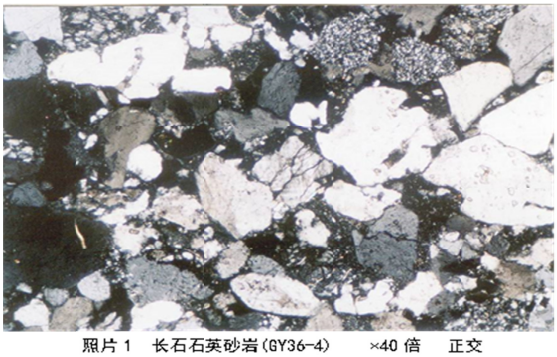

Fig. 4. Microstructures of glutenite samples

minerals in the ore include pyrite, albite, clay minerals, and organic matter. Uranium is primarily present in the form of adsorbed uranium and uranium minerals, with pitch uraninite and uranium black being the most common types of uranium minerals.

3.2. Rock physical and mechanical properties results and analysis

The results of the physical properties of the ore rocks are shown in TABLE 2. The physical parameters of the ore rocks show that the density of the ore rocks of this uranium deposit is 2.76-2.78 g/cm^3 for grains and 2.35-2.43 g/cm^3 for blocks, which confirms that the ore rocks are quartz-dominated gravels. The water content of the mineral rock is only 0.98-1.02%, indicating that the mineral rock has a low water content, which is consistent with the characteristics of a sparse and dry sand conglomerate. The porosity of the mineral rock is as high as 9.93-10.98%, which indicates that the mineral rock has high pore and fissure development, poor denseness and relatively low mechanical strength. The physical, chemical and mechanical properties of the mineral rock will change after encountering water, and the water absorption rate, saturation water absorption rate and water saturation coefficient are the indicators of the water absorption properties of the mineral rock. Mineral rocks with high water absorption tend to swell after encountering water, which affects the stability of the tunnel and causes tunnel damage. The softening coefficient characterises the degree of mechanical strength reduction. The softening coefficient of this mineral rock is 0.6-0.74, which is lower than 0.75, indicating that the mineral rock has poor engineering geological conditions, strong softening after encountering water, and weak resistance to water and weathering. The ore rock has a permeability measurement of 0.58-0.62×10-2 μm^2, indicating that it has good permeability and is suitable for conducting permeability tests and engineering practices.

TABLE 2

Physical parameters of ore and rock

No. specimen	Particle density (g/cm^3)	Bulk density (g/cm^3)	Softening coefficient Water content	Water absorption (%)	Water absorption rate (%)	Saturated water absorption rate (%)	Water-filled coefficients	Porosity (%)	Permeability (×10^{-2} μm^2)
XJPD-1	2.78	2.41	0.60	0.98	2.43	2.46	0.99	9.93	0.58
XJPD-2	2.77	2.38	0.71	1.02	2.49	2.52	0.99	10.25	0.59
XJPD-3	2.76	2.35	0.74	1.01	2.92	2.95	0.99	10.98	0.61
XJPD-4	2.77	2.43	0.72	1.00	2.42	2.45	0.99	9.96	0.58

The difference in mechanical parameters of the mineral rock before and after the action of the acidic solution is shown in TABLE 3. It indicates that the mechanical parameters of the mineral rock are significantly deteriorated, which is the result of the physicochemical interaction between the water and the rock. The physical action is mainly reflected in the lubricating and softening effect of the aqueous solution on the contact surface between the mineral particles or cement of the specimen, which reduces the friction factor and cohesion of the particle contact surface; the scouring, diffusion or transmission of the aqueous solution, which causes the loss of

material on the free surface of the mineral particles or cement of the mineral rock and produces secondary pores, which causes the change of the microstructure of the mineral rock. When water interacts with rock, it causes a chemical reaction that alters the size and mineral composition of the sandstone particles. This reaction also dissolves certain substances, which increases the porosity of the rock and makes it softer and less compact. Quartz, rock chips, feldspar and clastic cement composition.

The specimens used in the test consisted mainly of quartz, rock chips, feldspar and clastic cement. The most abundant quartz is the most stable and does not normally react chemically with aqueous solutions. The physical and chemical properties of the various rock chip aggregates are the most unstable and are easily lost and altered in underwater flow conditions. Feldspar can undergo ion exchange and hydrolysis under the action of aqueous solutions to produce new clay minerals. The secondary porosity of the rock is increasing due to the loss of clastic cement and the dissolution of feldspar, which is manifested as a decrease in cohesion and strength.

TABLE 3

Test results of rock mechanics parameters

No. specimen	Compressive strength (MPa)		Tensile strength (MPa)		Cohesive force (MPa)		Angle of internal friction (°)		Modulus of elasticity (GPa)		Poisson's ratio	
	natural	saturated	natural	saturated	natural	saturated	natural	saturated	natural	saturated	natural	saturated
XJPD-1	29.75	25.39	1.39	1.08	2.55	0	32.21	27.92	2.47	2.47	0.29	0.29
XJPD-2	17.41	10.42	0.79	0.57	1.51	0	31.38	27.47	1.46	1.46	0.32	0.33
XJPD-3	9.94	7.53	0.55	0.40	0.83	0.65	30.96	29.25	1.38	1.38	0.30	0.32
XJPD-4	15.30	11.30	0.83	0.56	1.29	0.96	32.21	30.54	1.43	1.43	0.32	0.32
XJPD-5	14.43	10.39	0.73	0.56	1.23	0.88	31.80	30.11	1.42	1.42	0.31	0.32

3.3. Simulation results and analysis

3.3.1. Stress analysis of the liquid collecting tunnel before and after leaching

The liquid collecting tunnel serves the purpose of gathering the leaching solution from the ore block. The redistribution of the stress field occurs after the excavation of the rock. From Fig. 5, with the excavation of the tunnel, the stress is continuously released and adjusted, and the surrounding rock is converging to the tunnel. The main stress value gradually increases; the two side walls of the liquid collecting tunnel show a large stress concentration, the top and bottom plate is the central tensile stress concentration area, and the two gangs are the compressive stress concentration area. The gradient of stress change gradually becomes smaller towards the periphery until it returns to the original rock stress state. Fig. 5 and Fig. 6 show that before leaching, the maximum principal stresses of Scheme 1, Scheme 2 and Scheme 3 are 7.92, 5.40 and 5.11 MPa, respectively, and the minimum principal stresses are 2.30, 1.83 and 1.84 MPa, respectively. The maximum and minimum principal stresses of Scheme 1 are 1.47 and 1.26 times those of Scheme 2, and 1.55 and 1.25 times those of Scheme 3, respectively. The stress values of Scheme 2 and Scheme 3 are very close to each other. After leaching, the maximum and minimum

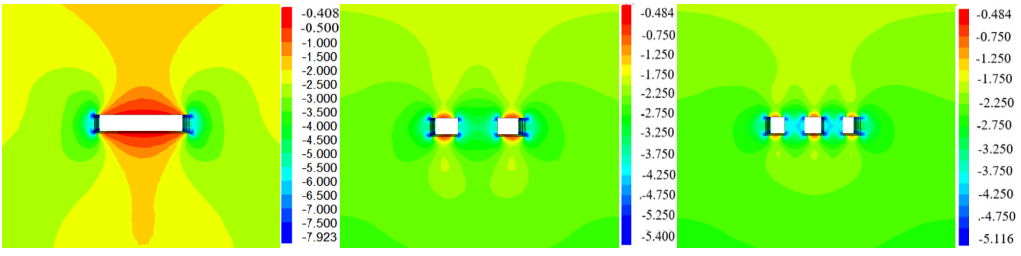

(a) Before leaching W = 10 m (b) Before leaching W = 3 m (c) Before leaching W = 2 m

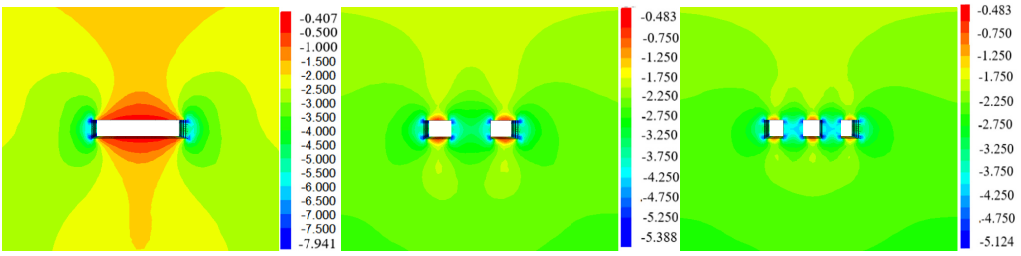

(d) After leaching W = 10 m (e) After leaching W = 3 m (f) After leaching W = 2 m

Fig. 5. Maximum principal stress distribution diagram of the tunnel with different structural parameters (MPa)

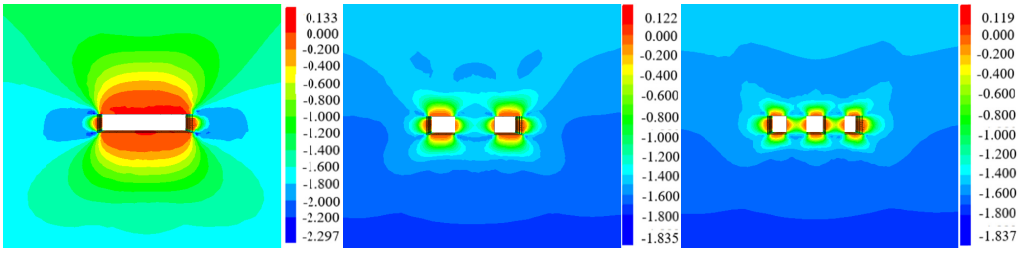

(a) Before leaching W = 10 m (b) Before leaching W = 3 m (c) Before leaching W = 2 m

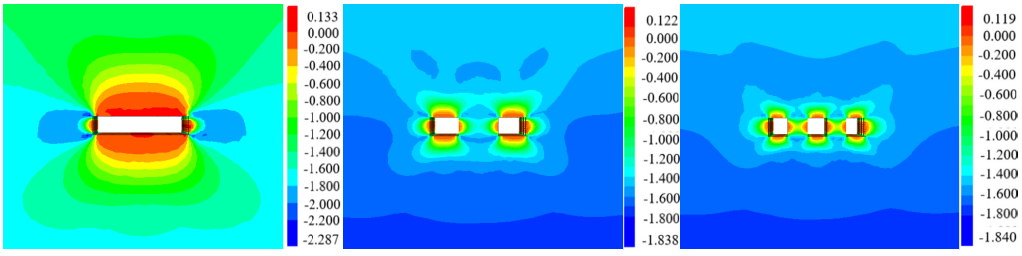

(d) After leaching W = 10 m (e) After leaching W = 3 m (f) After leaching W = 2 m

Fig. 6. Minimum principal stress distribution diagram of the tunnel with different structural parameters (MPa)

principal stresses of all three schemes do not change much from those before leaching, indicating that although the rock body shows a reduction in strength after leaching by the solution, it has a small effect on the stresses applied to the surrounding rock. In addition, it is worth noting that the top and bottom slabs of all three scenarios show positive stress values, which is tensile stress of 0.12-0.13 MPa before and after leaching and aiming to avoid rock destabilisation, the top and bottom slabs should be well supported in advance during excavation.

3.3.2. Analysis of collecting tunnel displacement before and after soaking

The amount of vertical displacement is a crucial factor to consider for the stability of the collecting tunnel. If there is too much displacement, it can result in the roof of the tunnel collapsing and the bottom gang bulging, which can make the tunnel unstable. Based on Fig. 7, before and after soaking, the overall displacement of the collecting tunnel is axisymmetric distribution, and the direction of movement of the surrounding rock all points to the void area of the tunnel, with the roof and floor of the tunnel forming displacement equivalence surfaces respectively; the central displacement of the top plate of the collecting tunnel is larger, and the displacement of the two bangs is smaller. With the increase in the width of the collecting tunnel, the central displacement of the top plate shows a gradual increase. Before soaking, the maximum vertical displacements of the three schemes are 11.2 mm, 3.7 mm and 2.9 mm respectively. What can be seen is that the vertical displacement of the rock body after excavation of scheme 1 is 3-4 times the deformation of the other two schemes, so scheme 1 is most likely to cause instability. The deformation of Scheme 2 is 1.3 times that of Scheme 3, and the two are relatively close. After

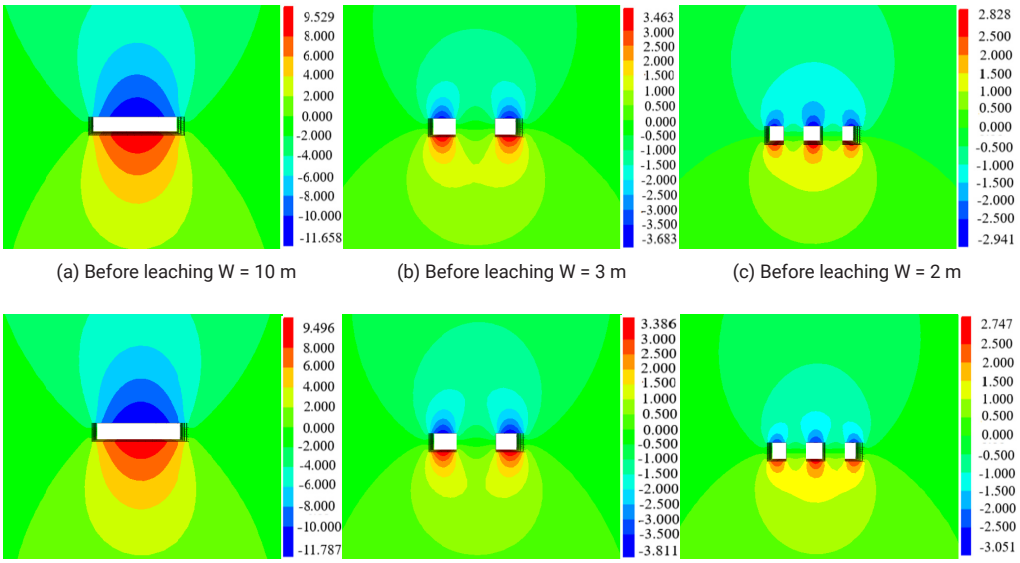

(a) Before leaching W = 10 m (b) Before leaching W = 3 m (c) Before leaching W = 2 m

(d) After leaching W = 10 m (e) After leaching W = 3 m (f) After leaching W = 2 m

Fig. 7. Vertical displacement distribution diagram of tunnel with different structural parameters (mm)

soaking, the maximum vertical displacements of the three schemes are 11.8 mm, 3.8 mm and 3.1 mm respectively, and the changes are 5.4%, 2.7% and 6.9% respectively, compared with those before soaking, which indicates that the dissolved soaking solution has a greater influence on the rock deformation, and the rock excavation size should be considered comprehensively after soaking the tunnel deformation.

3.3.3. Destruction state of plastic zone of collecting tunnel before and after leaching

The plastic zone is a phase where the strength and stability of ore rock diminish considerably, and harm to the plastic zone is a crucial indicator of destabilisation. Based on Fig. 8, after the excavation of the collecting tunnel, the exposed volume and area of the empty zone are increased, and the two gangs of the tunnel show a large plastic state, which is prone to plastic damage. Before leaching, shear damage and tension damage had already occurred in the two gangs of the collecting tunnel of scheme 1, and the plastic zone was enlarged after leaching. There is slight tension damage before leaching for scheme 2 and scheme 3, and after leaching, scheme 2 showed slight shear damage, while scheme 3 still had only tension damage. Since the actual excavation process will be supported, the tunnel size determined in accordance with plans 2 and 3 is relatively

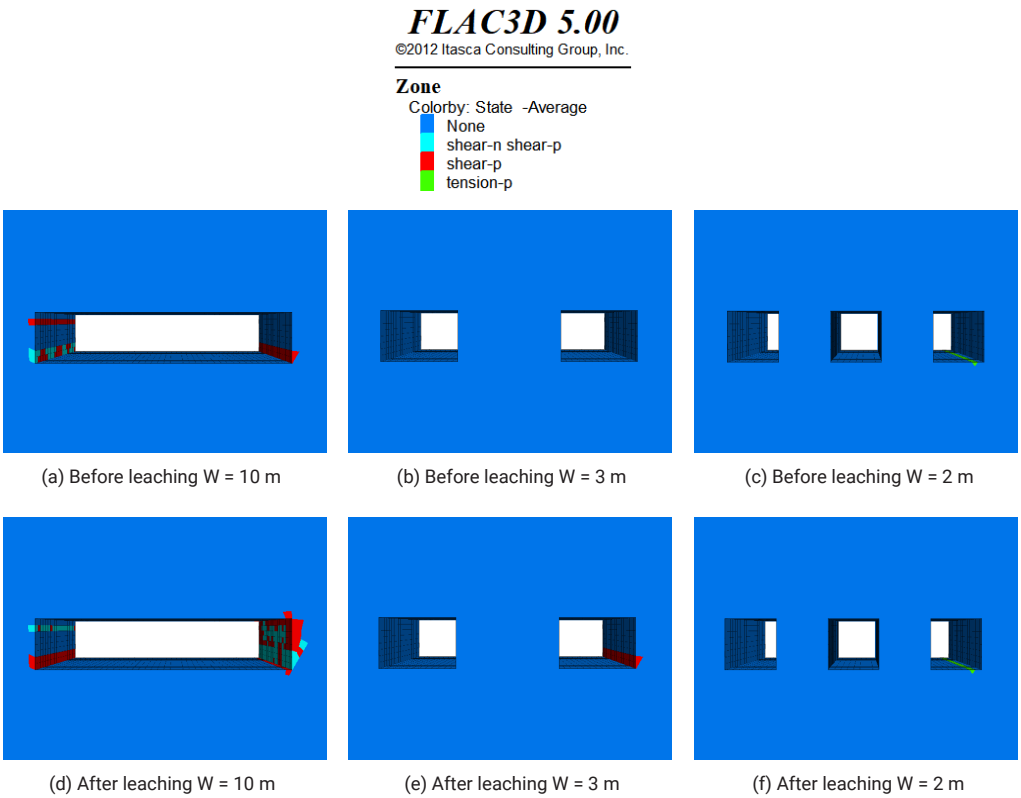

(a) Before leaching W = 10 m (b) Before leaching W = 3 m (c) Before leaching W = 2 m

(d) After leaching W = 10 m (e) After leaching W = 3 m (f) After leaching W = 2 m

Fig. 8. Distribution of plastic zone in tunnel with different structural parameters

safe for construction, while the top and bottom plates should be well maintained. Letter p represents a plastic state that occurred during the calculation. Letter n represents the plastic state that occurred after calculation, and the corresponding region is the plastic area.

4. Conclusion

(1) The physical properties of the rocks and the conditions of the ore body deposit indicate that this type of deposit is rare, typically steeply inclined sparse, and dry sand and gravel uranium deposit, which cannot be mined by the traditional ground soaking and in situ crushing soaking processes. A new economic, efficient and feasible process is a crucial way to realise the mining of this type of mineral. Theoretically, an underground in-situ leaching process can be used for mining this type of uranium deposit, but experimental studies are needed to obtain the necessary parameters for mining design before putting it into production. Using underground in-situ leaching to deal with those steeply inclined, sparse and dry sand is an original and innovative concept design. It is worthy of further study and related industrial tests.

(2) The mechanical parameters such as compressive strength, tensile strength, modulus of elasticity, inner cohesion and friction angle of the sand conglomerate after immersion in dilute acid solution show different degrees of reduction in comparison to the sand conglomerate in its natural state. The mechanism of water-physical action is mainly the softening of the contact surface or cement between mineral particles by the water solution and the secondary porosity and physical loss due to scouring, diffusion and transport; the water-chemical action mainly lies in the secondary porosity and water-chemical damage caused by the dissolution, dissolution and ion exchange of feldspar minerals and rock chips.

(3) Numerical simulation revealed that the maximum principal stresses in the collecting lane of three schemes, scheme I, scheme II and scheme III, before leaching was 7.92, 5.40 and 5.11 MPa, respectively, and the minimum principal stress was 2.30, 1.83 and 1.84 MPa, respectively, and the maximum vertical displacement was 11.2 mm, 3.7 mm and 2.9 mm, respectively with the range of plastic zone gradually becoming smaller; after leaching, the three the parameters related to the change of the alleyway of the three schemes have a similar pattern with those before leaching, and the main stress, maximum displacement and plastic zone all decrease as the structural parameters of the liquid collection alleyway shows a decrease. Before excavating the tunnel, it is important to support or reinforce the roof and floor beforehand.

(4) After conducting a thorough analysis of the safety and economic aspects of three different tunnel excavation schemes before and after leaching, it was discovered that Scheme I resulted in significant tension and shear damage due to its large exposed area and low safety factor. On the other hand, Scheme III had a high cost and poor economy despite its largeproduction of tunnel excavations. Upon comparison, it has been determined that Scheme II is the recommended option. This scheme involves arranging two liquid collecting tunnels along the strike of the ore body, with a tunnel size of 3 m ×2 m and a middle pillar width of 4 m. The numerical simulation results have important guiding significance for the design of the underground in-situ leaching process and the determination of structural parameters for this deposit.

Reference

[1] C.F. Zhang, B.S. Duan, R.S. Yang, Z.W. Yang, Z.R. Wang, Discussion on the mining method for a steep dip and unwatering sandstone uranium deposit in Xinjiang. Uranium Mining and Metallurgy **36** (4), 25 7(2017). DOI: http://doi.org/10.13426/j.cnki.yky.2017.04.004

[2] J. Sun, Rheological Behavior of Geomaterials and Its Engineering Applications, China Architecture and Building Press, Beijing 1999.

[3] H.H. Hu, B. Ye, Experimental Study on Mechanical Properties of Rock Creep in Saturation. Chinese Journal of Rock Mechanics and Engineering **21** (12), 1791-1796 (2002). DOI: http://doi.org/10.3321/j.issn:1000-6915.2002.12.009

[4] P. Li, J. Liu, G.H. Li, Experimental Study for Shear Strength Characteristics of Sandstone under Water-rock Interaction Effects. Rock and Soil Mechanics **32** (2), 380-386 (2011). DOI: http://doi.org/10.3969/j.issn.1000-7598.2011.02.010

[5] J. Liu, L.P. Qiao, P. Li, Experimental Studies and Constitutive Model of Elastoplastic Mechanical Behaviours of Sandstone with Hydro-physicochemical Influencing Effects. Chinese Journal of Rock Mechanics and Engineering **28** (1), 21-29 (2009). DOI: http://doi.org/10.3969/j.issn.1000-7598.2011.02.010

[6] L.S. Tang, S.J. Wang, Analysis of Mechanical and Quantitative Methods of Chemical Damage in Water-rock Interaction. Chinese Journal of Rock Mechanics and Engineering **21** (3), 314-319 (2002). DOI: http://doi.org/10.3321/j.issn:1000-6915.2002.03.004

[7] L.S. Tang, P.C. Zhang, S.J. Wang, Testing Study on Effect of Chemical Action of Aqueous Solution on Crack Propagation in Rock. Chinese Journal of Rock Mechanics and Engineering **21** (6), 822-827 (2002). DOI: http://doi.org/10.3321/j.issn:1000-6915.2002.06.012

[8] L.S. Tang, P.C. Zhang, S.J. Wang, Testing Study on Macroscopic Mechanics Effect of Chemical Action of Water on Rocks [J]. Chinese Journal of Rock Mechanics and Engineering **21** (4), 526-531 (2002). DOI: http://doi.org/10.3321/j.issn:1000-6915.2002.04.015

[9] L.S. Tang, C.Y. Zhou, Analysis of Mechanism of Permeation and Hydrochemical Action Resulting in Failure of Loaded Rock Mass. Acta Scientiarum Naturalium Universitatis Sunyatseni **35** (6), 95-100 (1996).

[10] Q. Cui, X.T. Feng, Q. Xue, Mechanism Study of Porosity Structure Change of Sandstone under Chemical Corrosion. Chinese Journal of Rock Mechanics and Engineering **27** (6), 1209-1215 (2008). DOI: http://doi.org/10.3321/j.issn:1000-6915.2008.06.015

[11] W. Wang, T.G. Liu, J. Lv, Experimental Study of Influence of Water-rock Chemical Interaction on Mechanical Characteristics of Sandstone. Chinese Journal of Rock Mechanics and Engineering **31** (2), 3607-3617 (2012).

[12] H.D. Jang, F.M. Qu, X.B. Liu, G.L. Zhang. Study on the Stability Evolution Law of Expansive Soft Rock Roadway Affected by Seasonal Wet-Dry Cycle. Archives of Mining Sciences **68** (1), 165-182 (2023). DOI: https://doi.org/10.24425/ams.2023.144323

[13] J.X. Wang, H.H. Zhu, Y.Q. Tang, Fracture Mechanical Model and Hydrochemical-hydraulic Coupled Damage Evolution Equation of Limestone. Journal of Tongji University (Natural Science) **32** (10), 1320-1324 (2004). DOI: http://doi.org/10.3321/j.issn:0253-374X.2004.09.002

[14] W.G. Li, X.P. Zhang, Y.M. Zhong, Formation Mechanism of Secondary Dissolved Pores in Arcose. Oil and Gas Geology **26** (2), 220-223 (2005).

[15] L.P. Qiao, J. Liu, X.T. Feng, Study on Damage Mechanism of Sandstone under Hydro-physico-chemical Effects. Chinese Journal of Rock Mechanics and Engineering **26** (10), 2117-2124 (2007). DOI: http://doi.org/10.3321/j.issn:1000-6915.2007.10.023

[16] L.P. Qiao. Experimental-theoretical-numerical Studies of Elasto-plastic and Creep Property of Sandstone with Hydrophysico-chemical Influencing Effects. PhD thesis, Chinese Academy of Sciences, Wuhan, 2008.

[17] N. Li, Y.M. Zhu, B. Su, S. Gunterc, A Chemical Damage Model of Sandstone in Acid Solution. International Journal of Rock Mechanics and Mining Sciences **40** (2), 243-249 (2003). DOI: https://doi.org/10.1016/S1365-1609(02)00132-6

[18] Z.H. Zhou, K.P. Hou, F.Y. Ren, Roof Stability Analysis of Sublevel Open Stope and Caving Mining Method. Journal of Mining and Safety Engineering **29** (4), 538-542 (2012).

[19] Z.H. Zhou, K.P. Hou, F.Y. Ren, Stability Analysis of Large-scale Mined-out Area and Its Control Methods in Paomaping Lead-zinc Deposit. Journal of Mining and Safety Engineering **30** (6), 863-867 (2013).

[20] G.Q. Tao, Q.Y. Ren, H. Luo, Stability Analysis of Stope in Pillarless Sublevel Caving. Rock and Soil Mechanics **32** (12), 3768-3779 (2011). DOI: https://doi.org/10.3969/j.issn.1000-7598.2011.12.038

[21] J. Gong, N.L. Hu, X.D. Wang, Stability Analysis and Rock Movement Prediction of Stope Roof Below the Subsidence Area. Journal of Mining and Safety Engineering **32** (2), 337-342 (2015). DOI: https://doi.org/10.13545/j.cnki.jmse.2015.02.026

[22] Y.P. Zhang, P. Cao, H.P. Yuan, Numerical Simulation on Stability of Complicated Goaf. Journal of Mining and Safety Engineering **27** (2), 233-238 (2010). DOI: https://doi.org/10.3969/j.issn.1673-3363.2010.02.019

[23] Y.M. Song, H. Ren, H.L. Xu, D. An. Experimental Study on Deformation and Damage Evolution of a Mining Roadway with Weak Layer Rock under Compression-shear Load. Archives of Mining Sciences **66** (3), 351-368 (2021). DOI: https://10.24425/ams.2021.138593

[24] A. Tajduś, K. Tajduś, Assessment of the Behaviour of Flysch Rock Mass During Tunnel Boring in the Primary Lining Using Indicators and Limit Values of Displacements and Deformations. Archives of Mining Sciences **67** (2), 355-376 (2022). DOI: https://doi.org/10.24425/ams.2022.141463

[25] Z.Y. Liu, M.K. Qin, H.X. Liu, Meso-Cenozoic Orogeny in South Tianshan and the Resultant Superimposed Enrichment Effect on the Sawafuqi Uranium Deposit. Acta Geologica Sinica **90** (12), 3310-3323 (2016).

[26] Geological and Mineral Industry Standard Drafting Group. Test Rules for Physical and Mechanical Properties of Rock (DZ/T 0276-2015). Standards Press of China, Beijing 2015.